Chapter 1: Introduction and Literature Review

Recent two decades are witness of vast interest in magnetic shape memory alloys (MSMAs) due to their large, fast, and recoverable magnetic field induced strain (MFIS) which could be directly utilized in the magnetic sensors and actuators [1-4]. Eventually, MSMAs emerge as an alternative to conventional shape memory alloys (SMAs) due to their large MFIS and fast switching which is beneficial for actuators [1]. Apart from the large MFIS, MSMAs show several other exotic phenomena like large magnetocaloric effect [5], giant magnetoresistance [6], anomalous thermal properties [7], exchange bias effect [8], spin-glass [9], strain glass [10], skyrmions [11], giant Hall effect [12] and anomalous Nernst effect [13], all of which have great potential for technological applications. The present thesis investigates the structural, magnetic, and anomalous transport properties of the two most important MSMAs, namely Ni_2MnGa and $Ni_{50}Mn_{34}In_{16-x}Al_x$ (x = 0.5, 0.8) as well as a related hexagonal NiMnGa system. Before going to review and details of Ni-Mn-based MSMAs and hexagonal MSMAs, some general phenomena (like martensite phase transition, shape memory effect, and premartensite phase) related to the present study are discussed below.

1.1 Martensite Phase Transition

Martensite phase transition (MPT) is a first-order, diffusionless phase transition wherein a material undergoes to a crystallographic change from high temperature and high symmetry cubic austenite phase to low temperature and lower symmetry martensite phase with tetragonal/orthorhombic/monoclinic structure [14-16]. MPT is well known in the steel wherein crystallographic change from austenite to the martensite phase has been visualized in the form of Bain distortion [17]. A schematic diagram of face centered cubic (FCC) austenite to body centered tetragonal (BCT) martensite transformation via Bain distortion is depicted in Figure 1.1 [16]. In

the parent FCC lattice with axes xyz, a BCT lattice with axes XYZ can be considered with tetragonality $c/a = \sqrt{2}$. If Z-axes contracted while X and Y-axes elongated so that c/a becomes the value of the martensite, then a BCT martensite phase is generated, as shown in Figure 1.1(b) [16]. This model of the lattice distortion was proposed by an American metallurgist E. C. Bain that is why this is known as Bain distortion [17]. Since MPT is a diffusionless phase transition driven by a shear-like mechanism, the direction and planes between the parent FCC lattice of austenite phase and BCT lattice of the martensite phase are related to each other for e.g., $[\bar{1}01]_A \parallel [\bar{1}\bar{1}1]_M$, $[\bar{1}\bar{1}2]_A \parallel [011]_M$, $(111)_A \parallel (011)_M$ in Figure 1.1(a) and (b), where subscripts A and M represent the austenite and martensite phases, respectively, while || indicates the equivalent [16].

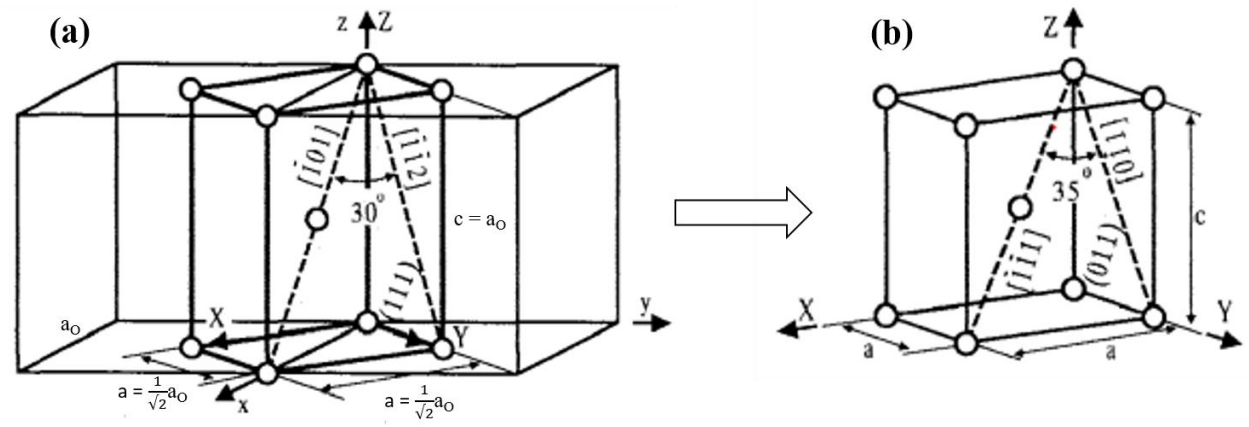

Figure 1.1: Schematic diagram of FCC austenite to BCT martensite transformation via Bain distortion. The xyz and XYZ represent the axes of the parent FCC austenite and BCT martensite phase, respectively. The lattice parameter (LP) of FCC lattice is labelled by a_O, while LP of BCT lattice are a and c [16].

In the MPT, the rearrangement of atoms takes place in an ordered manner; therefore, it is also known as displacive or military transformation [16]. The martensite phase is characterized by the development of a special microstructure formed by twinning or slip shear to accommodate the strain while maintaining the invariant habit plane [14-16, 18]. A typical schematic diagram of the

austenite to the martensite phase transition is shown in Figure 1.2(a), (b), and (c). A more simplified view of the parent austenite to the martensite phase transition is depicted in Figure 1.2(d), wherein the martensite in regions A and B have the same structure but have different crystallographic orientations. These regions (A and B) have been termed as variants of the martensite phase [16].

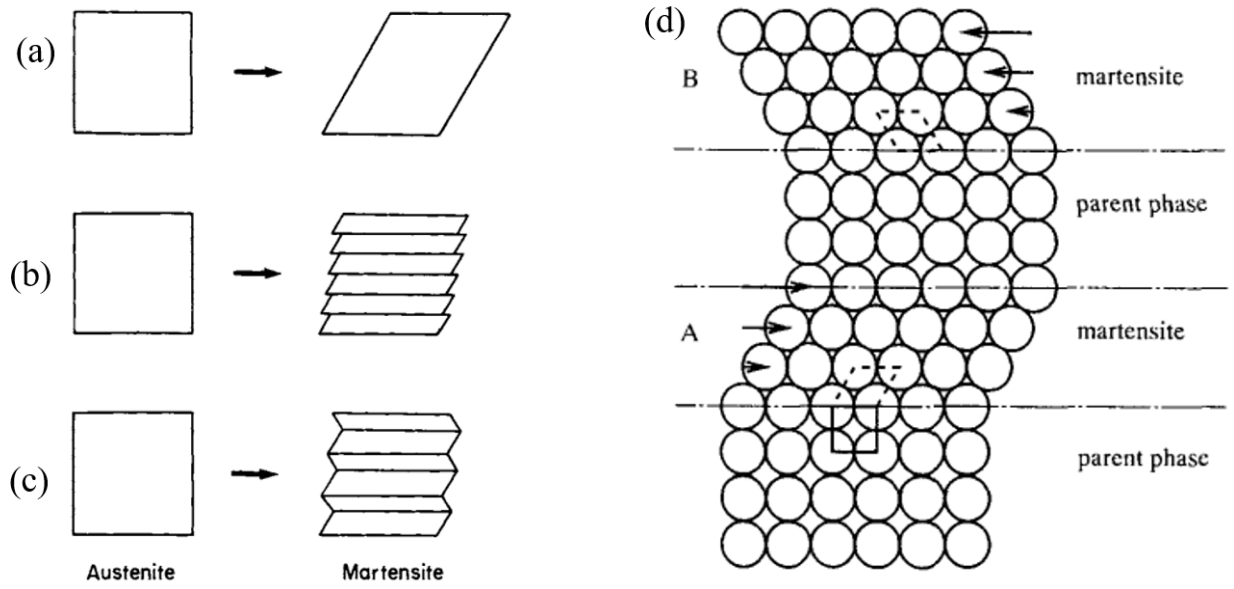

Figure 1.2: Lattice deformation from austenite to the martensite phase accompanying shear. (a) No lattice invariant shear, (b) Slip shear, and (c) Twinning shear [14]. (d) A more simplified model of austenite to the martensite phase transformation [16].

The characteristic temperature for the MPT can be defined as martensite start (M_s), martensite finish (M_f), austenite start (A_s), and austenite finish (A_f) with a characteristic thermal hysteresis during the cooling and warming cycle as depicted in Figure 1.3(a). In order to get the thermodynamical aspect of MPT, the variation of thermodynamic Gibbs free energy (G) with temperature for the parent austenite to the martensite transition is depicted in Figure 1.3(b), which

suggests that supercooling of temperature ΔT_s is necessary for the nucleation of the martensite phase.

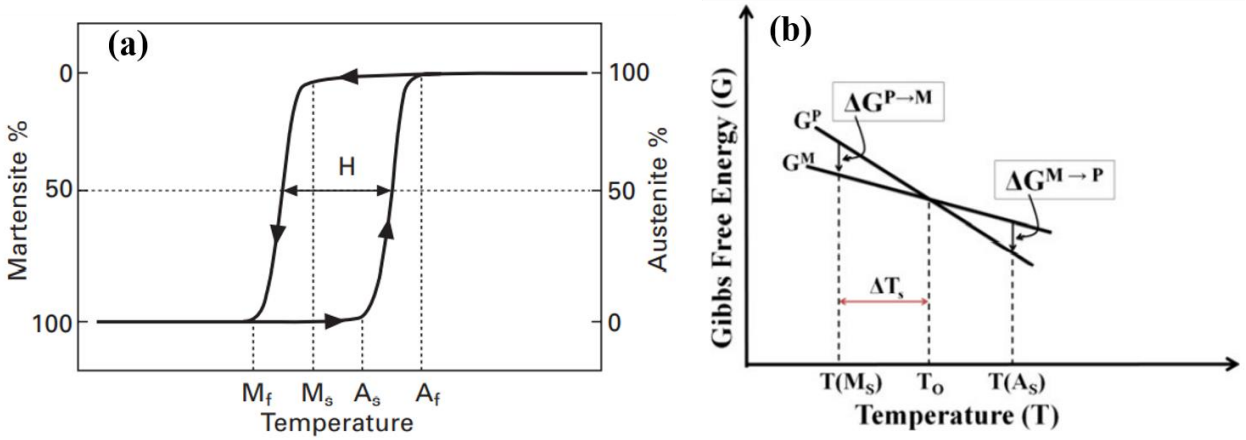

Figure 1.3: (a) Austenite to martensite phase transition with temperature change. The M_s, M_f, A_s, and A_f indicate the martensite start, martensite finish, austenite start, austenite finish temperatures, respectively. The H represents the width of the thermal hysteresis. (b) Schematic diagram of Gibbs free energy (G) relationship during the martensite transformation [19]. ΔT_s is the supercooling driving temperature for the forward martensite transformation. The subscripts P and M stand for the parent austenite and martensite phases, respectively, while T_O indicates the equilibrium temperature.

The MPT has been observed in various class of materials ranging from pure metals [20, 21] and alloys [14-16] to oxides [22], sulphides [23], ceramic [15, 16], polymers [24], and even in aminoacids [25, 26]. The MPT was first discovered in the steel, where it is irreversible and athermal [14]. In the athermal MPT, the fraction of the martensite phase depends solely on the temperature and remains constant with time. In contrast to the steel, a reversible MPT has been observed in the well-known shape memory alloys (discussed in section 1.2) like Ni-Ti [14-16, 27, 28], Ni-Al [14, 29, 30], where it may possess both athermal as well as isothermal characteristics

depending on the alloy composition under the application of temperature and stress [14, 16, 31]. In general, in the isothermal MPT, the fraction of the martensite phase increases with time at a fixed temperature.

1.2 Shape Memory Alloys

Shape memory alloys (SMAs) are a special class of materials, which remember their shape with the application of temperature and (or) load [15]. They return to their original shape from an inelastically deformed state upon heating to above a characteristic temperature which is known as austenite finish temperature (A_f). This phenomenon is known as the shape memory effect (SME). SMAs can also exhibit large recoverable shape changes by application and removal of external load above a characteristic temperature ($T > A_f$). This phenomenon is called superelasticity or pseudoelasticity [16]. These unique features of SMAs make them suitable for a wide range of applications in the technology for e.g., biomedical, robotics, aerospace, marine, energy conversion devices, textiles, sensors, and actuators for the next generation of micro-electromechanical systems (MEMS) [14-16, 32]. Although the Au-Pd was the first discovered SMA by Chang and Read in 1932 [33] the importance of SME was not realized until the discovery of NiTi (Nitinol) by Buehler *et al.* in 1962 [34]. The origin of the unique features of SMAs is related to the MPT [14-16]. The MPT is the hallmark of the large and reversible shape change in the SMAs, wherein different orientational variants of the martensite phase reorient themself in the direction of applied stress, and the original austenite state is recovered by heating to $T > A_f$ [14-16].

A pictorial representation of steps involved in the SME and superelastic behavior are shown in Figure 1.4, wherein austenite, twinned martensite, and detwinned martensite phases are depicted in (i), and (ii) and (iii), respectively. A reversible MPT appears between state (i) and (ii) on cooling up to temperature $T < M_f$ and heating back up to $T > A_f$ in Figure 1.4. In the twinned martensite

phase, there are martensite variants (indicated by X and Y) with different crystallographic orientations (indicated by arrow) in the state (ii) of Figure 1.4. The interface between X and Y is known as the twin boundary. The twinning arises to accommodate the strain energy in the martensite wherein the interface between martensite variant and parent phase remains undistorted, known as invariant or habit plane. The macroscopic shape of the twinned martensite phase (state (ii) of Figure 1.4) almost remains unchanged. On applying the external load along one of the martensite variants (let's say along Y-variant) in the state (ii), the X-variant gets aligned along the direction of external load via twin boundary motion and results in a detwinned martensite state (iii) with large shear strain. The macroscopic shape of state (iii) is different from the state (i) and (ii). On removing the load, the state (iii) does not revert back to the state (ii). Now, the shape of the state (iii) can be transformed to the original shape of the state (i) (austenite phase) on heating to $T > A_f$. This phenomenon ((i) to (ii) to (iii) to (i)) is known as SME. In addition, the state (i) can be directly transformed to state (iii) on the application of load and revert back to the state (i) on the removal of the load provided the temperature of the specimen should be $T > A_f$. This phenomenon is known as pseudoelasticity or superelasticity. For better visualization, the shape changes and shape recovery of a wire (see black curves in the states (i), (ii), and (iii) of Figure 1.4) are depicted.

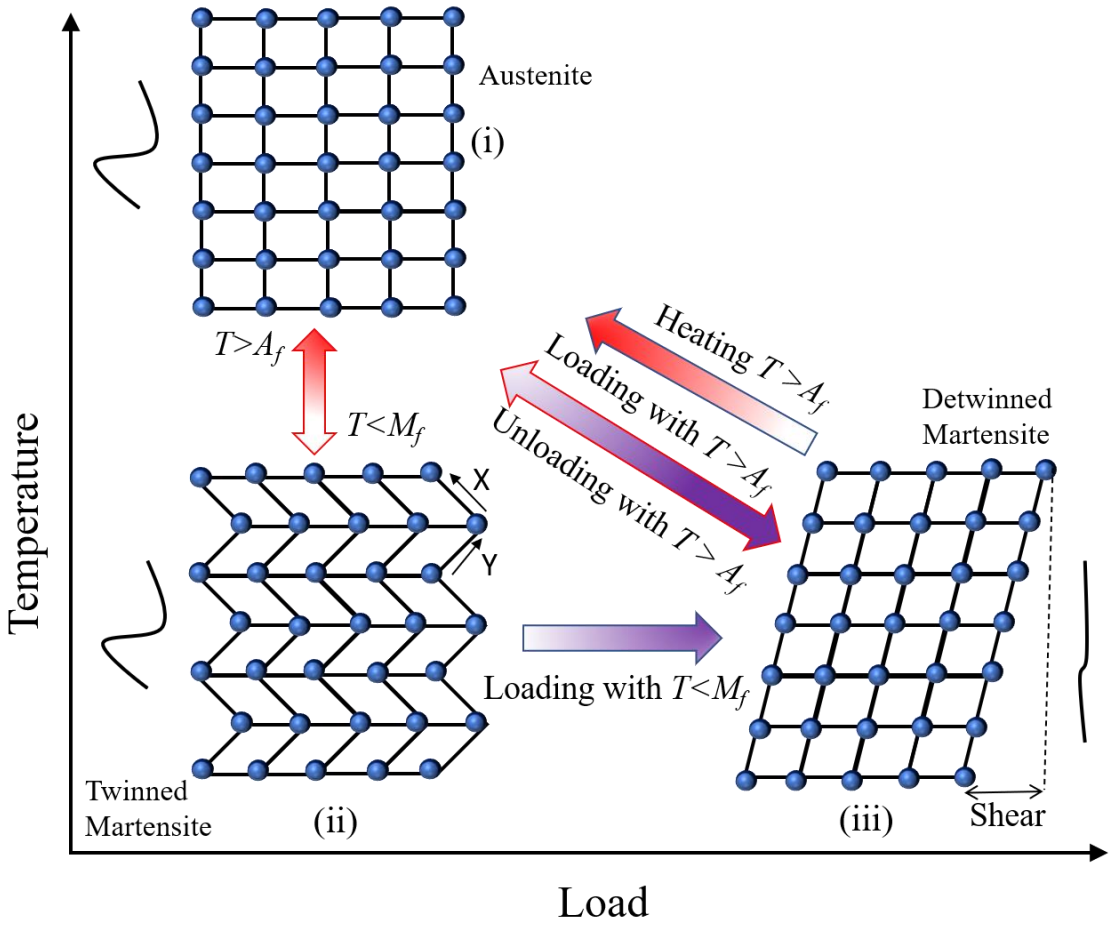

Figure 1.4: Schematic diagram of shape memory effect and superelastic behavior during cooling, heating, loading, and unloading are depicted. The states (i), (ii), and (iii) represent the austenite, twinned martensite, and detwinned martensite phases. Labels A_f and M_f indicate the austenite finish and martensite finish temperatures, respectively. The black curve represents a wire whose shape changes in (i) and (iii).

1.3 Magnetic Shape Memory Alloys

In recent decades, another kind of material known as the magnetic shape memory alloys (MSMAs) received tremendous attention due to its advantage over the conventional SMAs in the form of the larger magnetic field induced strains (MFIS) and faster switching [1, 2, 35-38]. In 1996, large

MFIS was discovered in single-crystalline Ni_2MnGa, which opened a new class of materials known as MSMAs [2]. The MFIS observed in Ni_2MnGa is comparable to the strain reported in one of the best magnetostrictive materials, such as Terfenol-D [39]. The MSMAs unleash a new pathway in the developing technology of sensors and actuators based on application/removal of magnetic field without any temperature change [1].

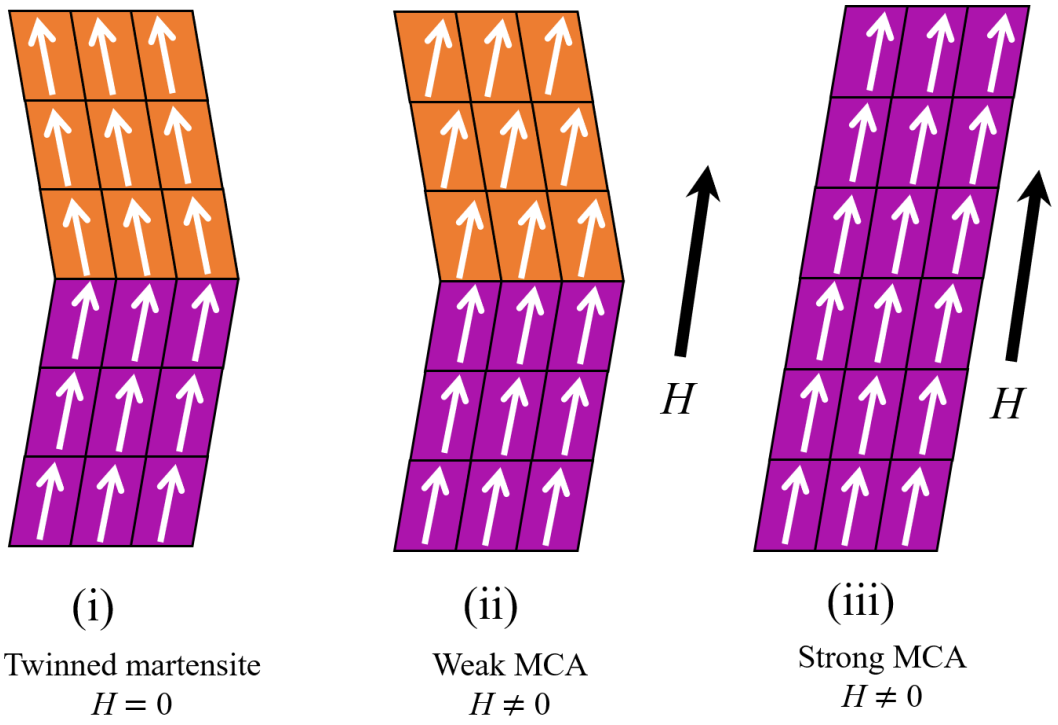

Figure 1.5: Schematic diagram of magnetic shape memory effect with application of magnetic field (H). The states (i), (ii), and (iii) represent the twinned martensite with no magnetic field, twinned martensite with field H, and detwinned martensite with field H, respectively. The MCA stands for magnetocrystalline anisotropy.

A pictorial representation of the magnetic shape memory effect (MSME) in the MSMA is shown in Figure 1.5. The mechanism of MSME is discussed as follows. In the first step, let us consider a twinned martensite variant with their crystallographic orientation as an easy axis of the

magnetization as depicted in the state (i) of Figure 1.5. The magnetic spins are aligned along the easy axis of the magnetization in the individual martensite variants. Now on the application of magnetic field along one of the directions of martensite variants may result in two cases depending upon the strength of magnetocrystalline anisotropy (MCA) denoted as K, and the twinning stress (σ_{tw}), which is the minimum stress or elastic energy required for the motion of the twin boundary. In the first case, if $K < \sigma_{tw}\, \varepsilon_0$ (ε_0 is the maximal strain), a simply reorientation of direction of magnetic spins of the individual martensite variants along the direction of the applied magnetic field with no net changes in the macroscopic shape (see the state (ii) of Figure 1.5) results on the application of magnetic field along one of the directions of martensite variants. In contrast, in the second case, if $K > \sigma_{tw}\, \varepsilon_0$, the twin boundary motion takes place in addition to the magnetic spin's reorientation along the applied field. Hence, the state (i) directly transformed to state (iii) in Figure 1.5, which exhibits large MFIS with net changes in macroscopic shape. The presence of sufficiently strong MCA ($K > \sigma_{tw}\, \varepsilon_0$) is the necessary condition for the MFIS. The difference between MCA energy and Zeeman energy of the adjacent martensite variants provides a driving force for twin boundary motion in the martensite phase. The twins with their easy magnetization direction along the applied field grow larger in comparison to the twins with other directions via twin boundary motion. However, removing the magnetic field state (iii) does not transform back to the state (i) unless there is external stress (σ_{ext}) applied perpendicular to the direction of the magnetic field. The stress σ_{ext} works as the restoring force in order to retrieve the shape into the original state (i) from the state (iii) in Figure 1.5. Thus, the necessary condition for reversible MFIS can be written as $K > (\sigma_{tw} + \sigma_{ext})\, \varepsilon_0$. It is worth mentioning here that the strength of σ_{ext} should not be large enough to block the field-induced motion of the twin boundary. In other words, the strength of σ_{ext} should not exceed a critical limit above which MFIS is completely suppressed.

Also, the strength of σ_{ext} should not be very small such that it is not able to revert back the strain. Thus, there is a critical value of the external stress, which is known as blocking stress, required for reversible MFIS.

There are several MSMAs for e.g., Fe-Ni [1], Fe-Pd [40], Fe-Pt [41], Ni-Mn-Z (Z=Ga, In, Sn) [2, 42-44], Co-Ni-Ga [45], Co-Ni-Al [46], Ni-Fe-Ge [47], Fe-Mn-Ga [48], etc. Among them, Ni-Mn-based MSMAs are mostly investigated as they show huge MFIS [3].

1.4 Ni-Mn-based Magnetic Shape Memory Alloys

The Ni-Mn-based MSMAs are of current interest due to their large MFIS and potential for technological applications such as magnetic sensors and actuators [2-4, 43, 49-51]. Apart from the large MFIS [2-4], the Ni-Mn-based MSMAs reveal several other exciting phenomena like large magnetocaloric effect [5, 52-55], giant barocaloric effect [56], giant magnetoresistance [6, 57-59], anomalous thermal properties [7, 60], exchange bias effect [8, 61], spin-glass [9], giant Hall effect [12] and anomalous Nernst effect [13], all of which have great potential for technological applications. These MSMAs have general formula X_2YZ, known as Heusler alloys [62]. For Ni-Mn-based MSMAs (or Heusler alloy), X and Y are represented by Ni and Mn, respectively, with Z = Ga, In, Sn, Sb [43].

1.4.1 Phase Transitions in Ni-Mn-Ga Magnetic Shape Memory Alloys

Among all Ni-Mn-based MSMAs, the Ni_2MnGa is the most studied MSMA, which exhibits huge (~10%) MFIS with reversible martensite phase transition at T_M ~ 220 K preceded by an intermediate premartensite (PM) phase transition at T_{PM} ~ 260 K, which will be discussed in detail in the section 1.4.3 [3, 63, 64]. Such a large MFIS of Ni_2MnGa has been suggested to be related with structural modulation of the martensite phase. The structural modulation can be derived from the basic structures having translation symmetry [65]. Structural modulation is basically the

modification in the periodicity of the basic unit cell along certain directions. If *n*-times modification in the lattice periodicity, then it corresponds to *nM* modulated structure, where *n* is a number of unit cells repeated to form superstructure [65, 66]. The modulated structures are generally described by a modulation wave vector **q**. If the magnitude of **q** is a rational number, then the superstructure is termed as a commensurate modulated structure. In contrast, if the magnitude of **q** is an irrational number, then the superstructure is known as an incommensurate modulated structure [65]. To visualize the structural modulation, a two-dimensional (2D) representation of the orientational relationship of unit cells between the parent austenite, premartensite (PM), and martensite phases are depicted in Figure 1.6 for Ni_2MnGa MSMA [66], wherein 3*M* modulated (inset (ii)), and 7*M* modulated (inset (iii)) unit cells are derived from the basic cubic cell by periodic displacement of (110) plane along $[1\bar{1}0]$ direction.

The large MFIS within the martensite phase of Ni_2MnGa is directly linked with the existence of a long period modulated structure, which provides lower twinning stress and facilitates the movement of twin boundary to achieve large recoverable strain [63, 67, 68]. Therefore, the nature and origin of structural modulation (in addition to their structure) has been a topic of intensive research in recent years [63, 69-79]. The nature of modulated structures and their origin in MSMAs are not only important to understand the large MFIS in these systems but also to improve other functional properties (like magnetocaloric effect and skyrmions) based on the martensite phase. The modulated structure of the martensite phase is the key factor behind the appearance of the reversible martensite phase transition [68, 80, 81], which is necessary for the utilization of these alloys in various technological applications for e.g., solid-state refrigeration and spintronic devices, where manipulation of structural and/or magnetic phases are required using magnetic field cycles [11, 82, 83].

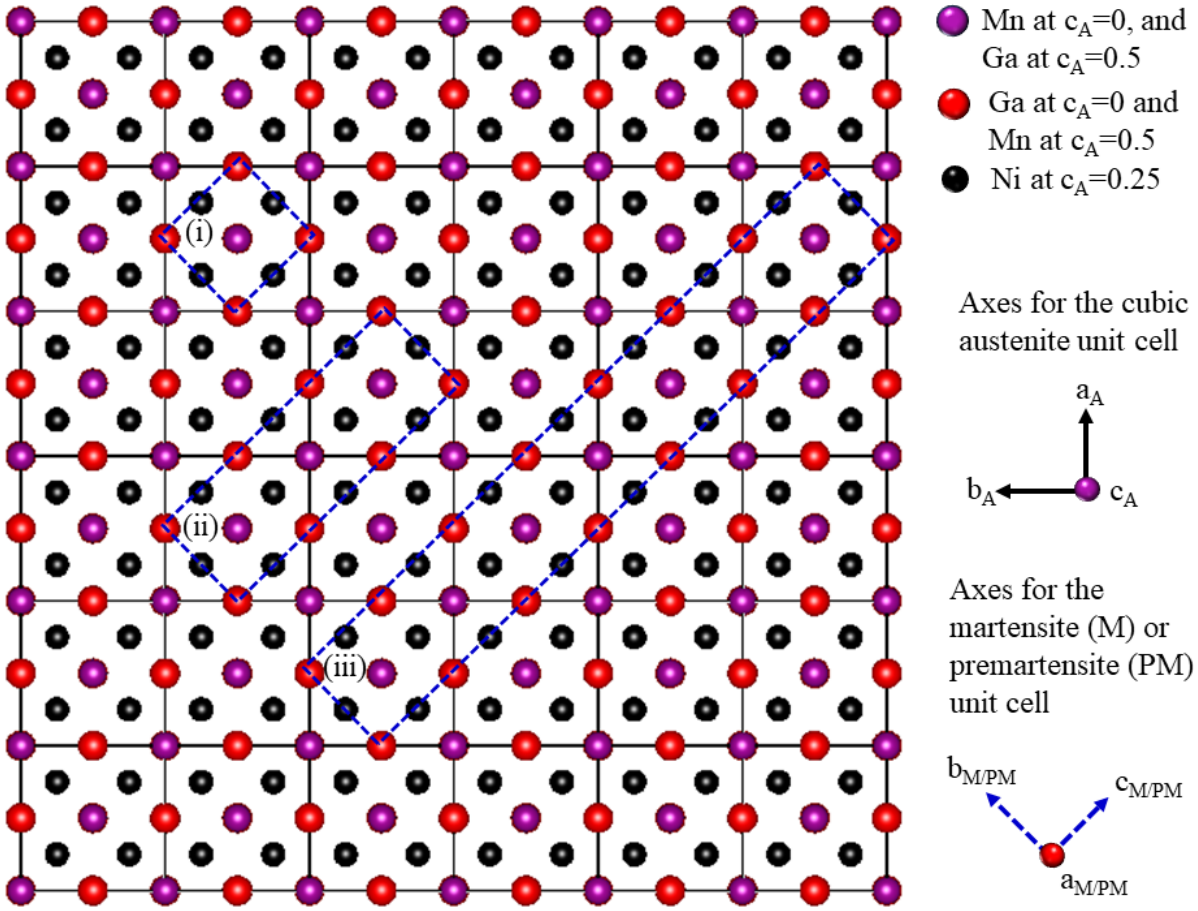

Figure 1.6: Schematic diagram of unit cells of austenite phase (A) for Ni_2MnGa MSMA. The inset (i), (ii), and (iii) depicts the unit cells of body centered tetragonal martensite, 3*M* modulated premartensite (PM), and 7*M* modulated martensite (M) phases, respectively.

In Ni_2MnGa, there has been lots of controversy on the nature structure modulation of the martensite phase, whether it is commensurate or incommensurate and 5*M* or 7*M* modulated [70, 84, 85]. Recently, a (3+1)D study using high-resolution SXRPD data revealed that the structure of martensite and PM phases is orthorhombic with incommensurate modulation of 7*M* and 3*M*, respectively [63, 71, 85]. In the literature, there are two different models have been proposed for the origin of structural modulation in Ni-Mn-based MSMAs. The first one is the adaptive phase model, which is based on a purely crystallographic scenario wherein the structure is visualized as

nanotwinned state of Bain distorted phase with the invariance habit plane between austenite and martensite phases to minimize the elastic energy [68, 76, 86, 87]. The second one is electronic structure-driven soft phonon-based model wherein modulation is linked with charge density wave (CDW) and softening of TA_2 phonon in the transverse acoustic branch along the [110] direction of the austenite phase due to Fermi surface nesting [63, 67, 71, 75, 77, 85, 88-90]. The soft phonon-based model supports the existence of the precursor PM phase. In contrast, the adaptive phase model does not support the existence of the PM phase. As per the recent study, the soft phonon-based model is most acceptable for the origin of the structural modulation in the Ni-Mn-Ga MSMAs [85, 90]. In contrast, the adaptive phase model has been proposed for the origin of structural modulation in Ni-Mn-In MSMAs (which will be discussed in detail in section 1.4.2) based on the strong evidence observed in high-resolution SXRPD and neutron powder diffraction study [91]. Nevertheless, more recently, the PM phase has also been reported in Ni-Mn-In MSMA [83]. This raises a question on the validity of the adaptive phase model in Ni-Mn-In MSMAs as the PM phase does not support this model. Thus, there are ongoing controversies regarding the origin of structural modulation in Ni-Mn-based MSMAs, which has remained unclear since the last three decades [76, 77, 92].

Although Ni_2MnGa shows huge MFIS, the martensite phase transition is ~210 K, which is far below room temperature. This hinders the direct application of Ni_2MnGa in real devices, wherein room temperature operating condition is required. Eventually, the structural as well as magnetic phase transitions temperature (and hence related properties) in these alloys have been observed to be very sensitive to their composition, as can be seen by the phase diagram of Ni-Mn-Ga given in Figure 1.7. In case of deficient Ni and excess Mn composition with valence electro concentration $e/a < 7.5$, the premartensite phase transition does not appear (see Figure 1.7(a)). In contrast, in the

case of excess Ni and deficient Mn composition with $7.5 \leq e/a < 7.58$, the premartensite phase transition appears at T_{PM} (see Figure 1.7(b)). Further, the premartensite phase transition appears at T_{PM} for excess Mn and deficient Ga composition with $7.4 \leq e/a < 7.58$ (see Figure 1.7(c)). Therefore, the composition tuning method has been opted to achieve the martensite phase at room temperature.

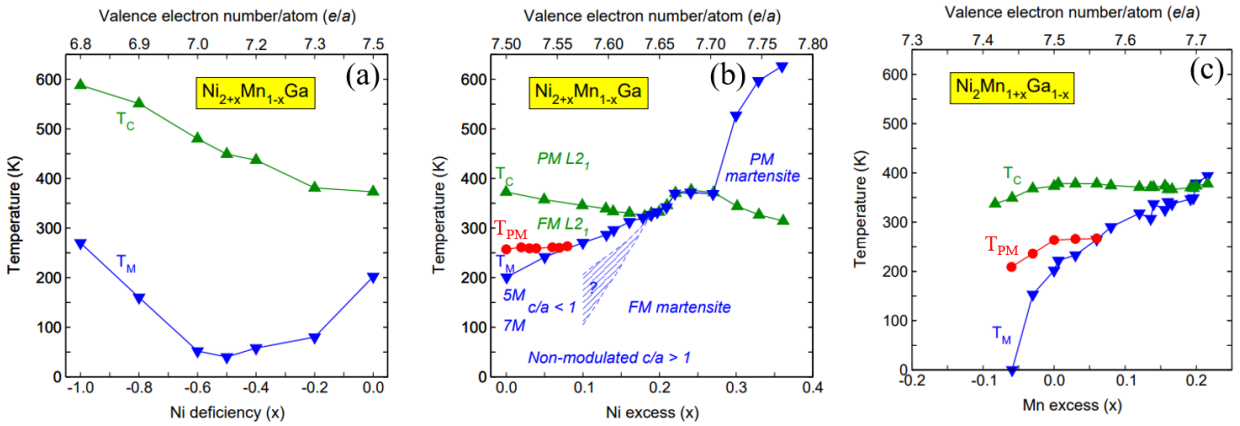

Figure 1.7: Phase diagram of Ni-Mn-Ga MSMA for (a) deficient Ni and excess Mn, (b) excess Ni and deficient Mn and (c) excess Mn and deficient Ga composition. The *FM* and *PM* stand for ferromagnetic and paramagnetic, while T_C, T_M, and T_{PM} indicate the *PM* to *FM*, martensite, and premartensite phase transition temperature, respectively [93].

However, Ni-Mn-Ga MSMAs show large MFIS; their output stress is limited (lower than 5 MPa). In addition, the heavy brittleness of this material puts a question mark on its applicability in the devices. Further, since ferromagnetic ordering is present in the austenite as well as martensite phases, a large magnetic field requires to field-induced phase transition as saturation magnetization of martensite and austenite phases are comparable. These drawbacks of Ni-Mn-Ga MSMA demand an alternative [94]. In 2006, large output stress (above 100 MPa) was reported in another kind of

MSMAs which is Ni-Mn-In [42]. This discovery revolutionized the In-based MSMAs, which are discussed in detail as follows.

1.4.2 Phase Transitions in Ni-Mn-In Magnetic Shape Memory Alloys

The In-based compositions (i.e., Ni-Mn-In MSMA) can be obtained by considering Z as In element in the Ni-Mn-Z. The standard Heusler composition Ni_2MnIn does not show martensite or PM phase transitions [95, 96], in contrast to the Ni_2MnGa. Interestingly, increasing the Mn content up to a critical value ($Ni_2Mn_{1.36}In_{0.64}$), starts to show the martensite phase transition [96]. The martensite phase exhibit 3*M* or 5*M* or 7*M* modulated monoclinic structure in Ni-Mn-In MSMA [43, 91]. There are only a few reports on the observation of the PM phase in Ni-Mn-In MSMAs [83]. A recent study suggests that the PM can be stabilized in Ni-Mn-In MSMAs by chemical pressure tuning [97]. In contrast to the Ni-Mn-Ga, the martensite phase of Ni-Mn-In MSMAs exhibits the lower magnetization state due to paramagnetic or antiferromagnetic ordering [96]. Also, it contains competing ferromagnetic and antiferromagnetic interactions in the martensite phase below a certain temperature (T_g) [91]. This competing interaction leads to interesting phenomena like exchange bias and spin-glass in Ni-Mn-In MSMAs. The structure, as well as magnetic transition temperatures and related properties of these MSMAs, are very sensitive to the composition and valence electron concentration per atom (*e/a*) ratio [98], as can be seen in the phase diagram of Ni-Mn-In MSMAs given in Figure 1.8 which suggest that martensite start temperature (M_s) can be tuned ranging from ~200 K to ~1000 K with increasing *e/a* ratio from ~7.85 to ~8.5.

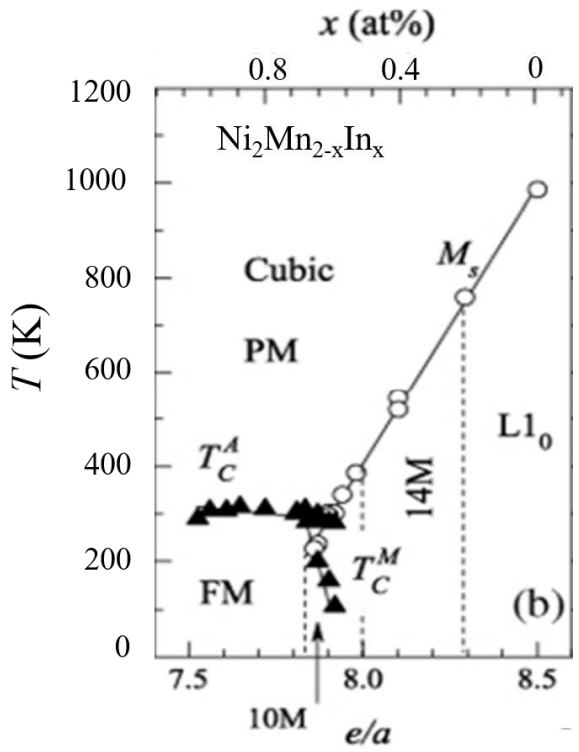

Figure 1.8: Phase diagram of Ni-Mn-In MSMA. The FM and PM stands for ferromagnetic and paramagnetic while T_C^A, T_C^M and M_s indicate the Curie temperature of the austenite, Curie temperature of the martensite, and martensite start temperature, respectively. Label $L1_0$ represents the $L1_0$-type tetragonal structure [98].

1.4.3 Premartensite (Precursor) Phase in Ni-Mn-based Magnetic Shape Memory Alloys

Apart from the martensite phase, another interesting feature, known as precursor effect or premartensite (PM) phase transition, occurs in the parent austenite phase and has been observed in well-known SMAs for e.g., Ni-Ti [27] and Ni-Al [99]. Precursor effects reflect in such a way that system prepares itself for actual phase transition [100]. The PM phase has been considered as an important precursor phase of the martensite phase in the important SMAs (Ni-Ti [27] and Ni-Al [99]) and MSMAs (Ni-Mn-Ga [88] and Ni-Mn-In [83]). In these alloys, the martensite phase does not appear directly from the high-temperature cubic austenite phase but is preceded by an

intermediate PM phase [63, 83, 88, 97, 100-104]. In other words, the PM phase appears at an intermediate temperature range between the high temperature cubic austenite phase and the low temperature low symmetry martensite phase with preserved symmetry of the cubic austenite phase, unlike the symmetry breaking martensite phase transition [105-111]. Initially, the precursor effect was understood in the form of premonitory effects observed by softening of certain elastic constants prior to martensitic phase transformation [112]. Since the PM phase is directly related to the martensite phase, which is the heart of SMAs and MSMAs to show SME, the PM phase has received tremendous attention in these alloys from the point of view of crystal structure, phase stabilities, understating of structural modulation and structure-property relation [63, 88, 99, 109, 112-124]. A detailed study of the precursor PM phase is necessary to explore the exotic physical properties like strain glass [10], and skyrmion [83] recently observed in the MSMAs as these properties are directly related to the PM phase. The strain glass is another fascinating phenomenon where short-range ordered strain remains hidden in the random long-range strains [10, 124-132]. The strain glass is analogous to the spin-glass [133], dipole glass [134] and relaxor [135]. The details of skyrmions are described in the section 1.5.

In general, the appearance of the PM phase accompanies structural modulation in SMAs and MSMAs. For example, the precursor PM state in nearly stoichiometric or off-stoichiometric Ni-Ti or Fe-doped Ni-Ti [14, 16, 27, 112, 136] SMAs have been characterized by the presence of diffuse scattering around the incommensurate positions of the trigonal structure (i.e., 3R) [27, 74, 106, 137-140]. At lower temperatures, this precursor PM state transformed to another long-range ordered PM phase [106], which is also known as R-phase or R-martensite phase [27, 130, 131] with a trigonal structure in the space group $P\bar{3}$ [28, 116]. In Ni_2MnGa MSMA, the PM phase exhibits an orthorhombic structure with 3*M* modulation as depicted in the inset (ii) of Figure 1.6

[71]. The origin of the PM phase and its relation with the martensite phase have remained a topic of debate in both SMAs and MSMAs for a long time and have not been well understood yet [71, 73, 88, 100, 104-106]. It has been proposed that the PM originated by electron-phonon coupling and Fermi surface nesting feature in SMAs [105]. However, in the MSMAs, magnetoelastic coupling has been proposed as one of the key factors for stabilizing the PM phase with significant magnetic field dependency of PM phase transition temperature [100, 102, 141].

In general, the feature of PM phases appears very weak, which makes the most of the techniques of the conventional experiments for e.g., magnetization [63], resistivity [60], electron microscopy[39], high-resolution synchrotron x-ray diffraction [63], photoemission spectroscopy [90], softening of elastic constant [142], etc., to show only weak sensitivity (or sometimes insensitivity) across the PM phase. Apart from these techniques, inelastic neutron scattering (INS) is one of the excellent techniques to detect precursor PM phase by obtaining the phonon dispersion curves [88, 105, 143]. In the INS signal, the existence of the precursor phase is interpreted by the presence of minima/dip in the energy of the certain mode of dynamic lattice vibration at a specific wave vector [88, 105]. The energy/frequency of this certain mode of vibration gets decreases on lowering the temperature (ongoing toward transition temperature), which is termed as phonon softening [88, 105], and that particularly associated mode is known as a soft mode. Generally, the PM phase is associated with incomplete phonon softening [105, 118, 139]. In phonon softening, the phonon frequency decreases on decreasing the temperature toward the transition temperature according to standard soft mode theory [144, 145]. In complete phonon softening, the frequency almost tends to zero as the transition temperature approaches, corresponding to the lattice instability. Hence, the structure transforms to a different phase with different symmetry from the parent phase. After that, phonon frequency starts to increase (hardening). This leads to complete

phase transition and is generally observed in the second-order in nature [144, 145]. In an incomplete phonon softening, the phonon frequency remains finite at the transition temperature point and is generally associated with weakly first-order phase transition. For example, in the case of well-known Ni_2MnGa MSMA, PM phase transition occurs before the phonon frequency can reach zero value, and hence phonon frequency started to rise below actual PM phase transition temperature (T_{PM}) [146]. The lattice instability near the transition point leads to PM phase transition, which turns to increase the phonon frequency instead of further decreasing (softening) below T_{PM} i.e., incomplete phonon softening.

Although PM phase was considered as the precursor state of the martensite phase with preserved cubic symmetry of the austenite phase [99, 100], a recent high-resolution synchrotron x-ray diffraction study revealed the robust Bain distorted thermodynamic stable PM phase in $Ni_{1.9}Pt_{0.1}MnGa$ MSMA and proposed that PM phase should not be considered as the precursor state of the martensite phase [123]. Therefore, a natural question arises: is there any precursor state of the PM phase? In Ni-Mn-Ga, the precursor effect has been realized in the form of tetragonally distorted local nanoregions in the parent austenite phase by the diffuse scattering measurement [147]. Further, the local nuclear magnetic resonance (NMR) study of Ni_2MnGa provided evidence for the precursor of the martensite phase well inside the parent austenite phase [148]. Although these precursor effects have been suggested to be the precursor of the martensite phase [147, 148], the INS experiments reveals precursors in the form of diffuse scattering and softening of 1/3 (110) transverse acoustic (TA_2) phonon mode and suggest that the precursor effects in the parent austenite phase of Ni_2MnGa are related to the PM phase [88]. Thus, an ongoing controversy calls for a direct structural investigation of such precursors in Ni_2MnGa MSMA. In addition, as discussed above, PM occurs in a narrow temperature range with signature in the conventional

experiments. Therefore, a stable PM phase in a wide temperature range is required for a more profound PM phase investigation.

It has been proposed that the PM phase is directly related to the skyrmion formation (and hence, related Hall effects) in the Ni-Mn-based MSMAs [83]. Therefore, it is important to investigate the Hall effect in Ni-Mn-based MSMAs. There are only a few reports of the Hall effect, whose origin remained a matter of concern, especially in the Ni-Mn-Ga MSMAs, as they exhibit multiple phase transitions (austenite, martensite, and PM phase) [149, 150]. The details of the Hall effect are given in the upcoming section 1.5.

1.5 Anomalous and Topological Hall Effect

Hall effect is the phenomenon wherein the presession of electrons takes place along one side of a current-carrying conductor placed in a perpendicular magnetic field due to the Lorentz force [151]. The presession of electrons along one side of the conductor enables the appearance of an effective transverse (or Hall) voltage along the side of the conductor, and results to an effective Hall resistivity. The Hall resistivity (ρ_{xy}) is proportional to the applied magnetic field (H) i.e., $\rho_{xy} = R_0 H$, where R_0 is the ordinary Hall coefficient. A typical schematic of the Hall effect and variation of resistivity with the field is depicted in Figure 1.9. Edwin H. Hall discovered the Hall effect in 1879, and since then, it has received tremendous interest due to its direct applicability in the technology for making various devices like Hall sensors, magnetometers, as well in basic physics understanding like determination of type and mobility of charge carriers and their concentration, which revolutionized the semiconductor technology [151].

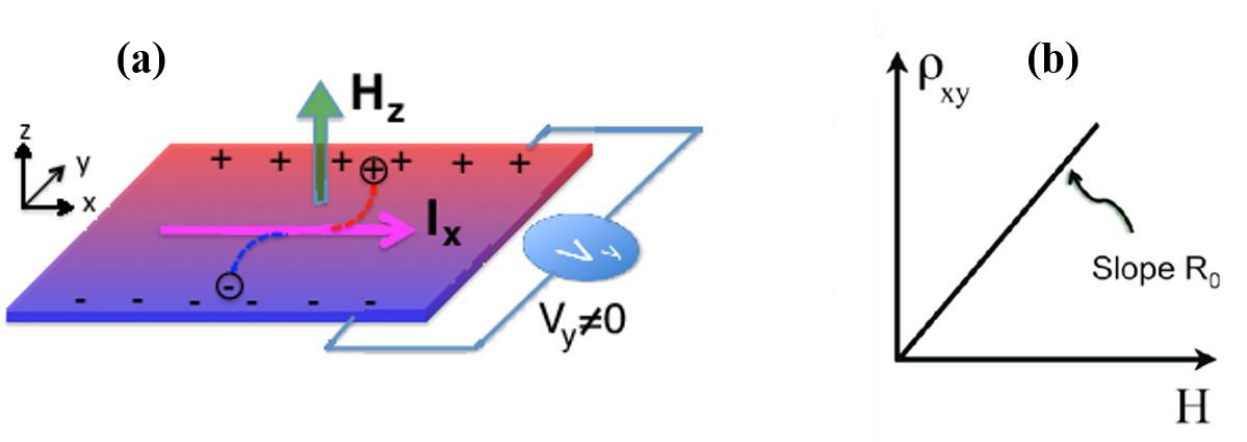

Figure 1.9: (a) Schematic illustration of Hall effect, where I, H, and V stand for current, magnetic field, and Hall voltage, respectively [152] and (b) Hall resistivity (ρ_{xy}) with magnetic field for a nonmagnetic conductor [153].

Later, Edwin H. Hall observed the ten times stronger presession of electrons in the ferromagnetic (FM) conductor in comparison to the nonmagnetic conductor [151]. Subsequently, this stronger effect in the FM materials is named as anomalous Hall effect (AHE). In the FM materials, the AHE is an additional Hall resistivity (R_sM) in addition to the ordinary Hall resistivity (R_0H) corresponding to the ordinary Hall effect (OHE) [151, 154, 155], i.e.,

$$\rho_{xy} = R_0H + R_sM \quad \ldots(1.1)$$

where R_s and M are anomalous Hall coefficient and magnetization, respectively [151]. A typical schematic of anomalous Hall effect and variation of ρ_{xy} with field are depicted in Figure 1.10. It is evident from Figure 1.10(b) that initially, ρ_{xy} increases with the field, and after a certain field, it tends to saturate analogous to the magnetization due to the second term in eq. (1.1) corresponds to AHE, but the first term in eq. (1.1) continues to grow with the field. In the recent past, the AHE has received tremendous interest due to its potentiality as a new generation of conventional electronics in the form of spin-based memory devices for e.g., magnetic random access memory

(MRAM) devices in spintronics [151, 156], spin orbitronics [157] as well as in the fundamental physics to understand the topological band structure, spin polarization of current carriers [12], etc.

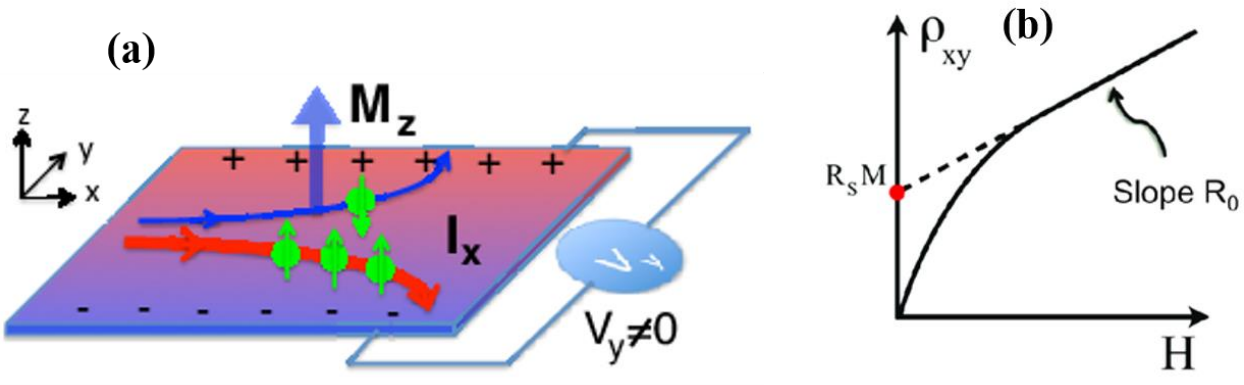

Figure 1.10: (a) Schematic illustration of anomalous Hall effect (AHE) [152] and (b) Hall resistivity (ρ_{xy}) with magnetic field for a ferromagnetic conductor, where $R_S M$ is the zero-field intercept and is related to the AHE (see eq. (1.1) for more detail) [153].

Although it was believed for a long time that AHE scales with magnetization (i.e., proportional to the magnetization) of FM materials, subsequently, it was realized that the electronic band structure of the materials could impact the AHE significantly [151, 158]. The origin of AHE is related to the joint interaction of spin-orbit coupling (SOC) and magnetization [151, 154, 155]. Three mechanisms have been proposed to understand the AHE in the magnetic material. These mechanisms are intrinsic (scattering independent), skew scattering, and side jump [151]. The SOC plays a vital role in these mechanisms responsible for the AHE. The different mechanisms to the AHE are depicted in Figure 1.11.

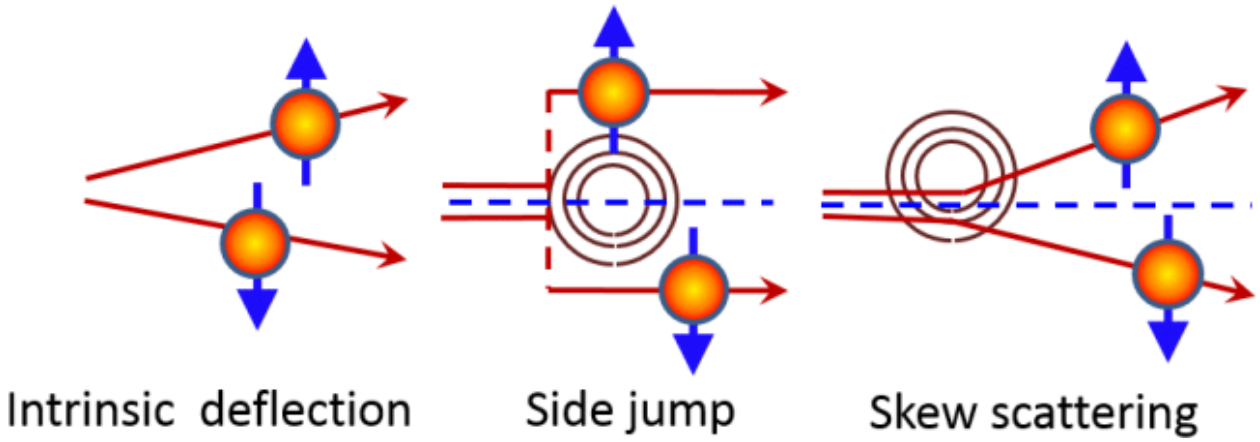

Figure 1.11: Schematic illustrations of intrinsic, side jump, and skew scattering mechanism to anomalous Hall effect [159].

The intrinsic mechanism was explained by Karplus and Luttinger's theory in 1954 [160], subsequently interpreted through momentum space Berry phase and Berry curavture [161], which purely depends on the electronic band structure of the materials. The Berry curvature acts like a pseudomagnetic field in the momentum space. This pseudomagnetic field provides an anomalous velocity to the conducting electrons perpendicular to the applied electric field and thus resulting in the AHE, even in the absence of an external magnetic field [162]. The skew scattering and side jump have been classified in the scattering-dependent extrinsic mechanism caused by the scattering of conduction electrons with magnetic impurities in the FM material [151, 163]. In order to distinguish the different mechanisms, the scaling relation has been derived between anomalous Hall resistivity (ρ_{xy}) and longitudinal resistivity (ρ_{xx}) for e.g., the scaling relation is $\rho_{xy} \propto {\rho_{xx}}^2$ for the intrinsic and side jump mechanisms while it is $\rho_{xy} \propto \rho_{xx}$ for the skew scattering mechanism [163]. Identification of the major contribution of the different mechanism to the AHE is still a subject of intense debate in the different materials and require detailed studies [157, 163].

In addition to the AHE, another fascinating topological Hall effect (THE) received tremendous interest in recent years [164-167]. In addition to the OHE and AHE, THE is an extra contribution (known as topological Hall resistivity; ρ_{xy}^{T}) in the total Hall resistivity i.e.,

$$\rho_{xy} = R_0 H + R_s M + \rho_{xy}^{T} \ldots (1.2)$$

This ρ_{xy}^{T} appears due to the fictitious magnetic field induced by the Berry curvature in real or momentum space when the conduction electrons interact with chiral noncoplanar magnetic spin textures like skyrmions [166, 168, 169] depicted in Figure 1.12. When maximum value to ρ_{xy}^{T} is independent of ρ_{xx} (or temperature) then THE is induced by real space Berry curvature [169, 170]. In contrast, when maximum value to ρ_{xy}^{T} depends on ρ_{xx} then THE is induced by momentum space Berry curvature [169]. THE is the hallmark for the noncoplanar structures with non-zero spin chirality as well as topologically protected magnetic skyrmions [165-167], which are the particle-type swirling of magnetic spins around the unit sphere in a nanometer scale. The skyrmions received tremendous attention due to developing factor in high-density information carriers, data processing, and memory devices [162, 171-174] for their unique properties such as the nanometer size, topological stability, and low power consumption (low current density ~$10^5 - 10^6$ A-m^{-2}) [175-177]. Initially, the skyrmions were observed in non-centrosymmetric systems for e.g., B20 magnets like MnSi [178], MnGe [179], FeGe [180], Cu_2OSeO_3 [181], etc., due to the competition among Heisenberg exchange interactions, Dzyaloshinskii-Moriya interactions (DMI) and magnetic anisotropy [182, 183].

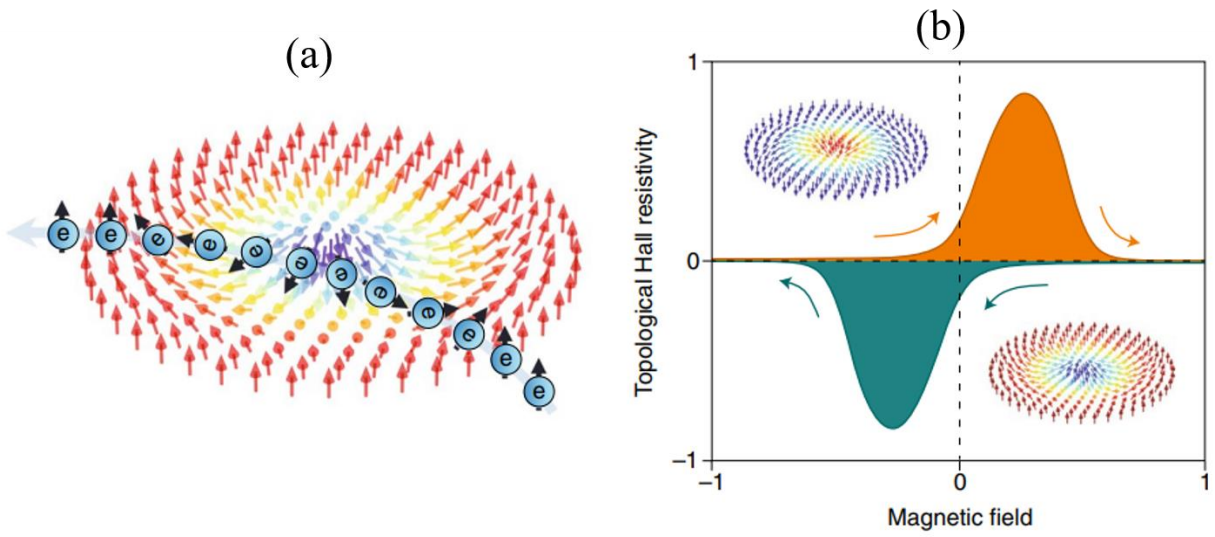

Figure 1.12: The schematic diagram of topological hall effect (THE). (a) Turning of electron trajectory on passing through a magnetic texture like skyrmion. The electron's spin orientation follows the spin orientation of the skyrmion texture. (b) Topological hall resistivity vs magnetic field plot, where arrow indicated the direction of field sweeping. Insets in (b) show positive and negative magnetic fields skyrmions with reversed spin texture [184].

Later, skyrmions were also discovered in the centrosymmetric systems with inversion symmetry [11, 185, 186] for e.g., NiMnGa [187], $La_{2-2x}Sr_{1+2x}Mn_2O_7$ [185], MnPdGa [188], NiI_2 [189]. The magnetocrystalline anisotropy plays a vital role in stabilizing the magnetic skyrmions due to competing interactions between magnetic anisotropy energy and dipolar interactions energy in the centrosymmetric materials [11, 185, 187]. THE has been widely investigated in B20 magnets [167, 177, 190, 191] and other systems having skyrmions [187, 192] or non-trivial spin textures with nonzero spin chirality [162, 170]. More recently, a large THE induced by skyrmions or by nonzero spin chirality has been observed in noncentrosymmetric Heusler compounds with D_{2d} crystal symmetry for e.g., Mn_2NiGa [165], Mn-Pt(Pd/Rh)-Sn [166, 193, 194], Mn-Pt-In [195]. In contrast, there are only a few reports on the presence of skyrmions in the centrosymmetric Heusler

compounds, which shows magnetic shape memory effect for e.g., Ni_2MnGa [11] and $Ni_{50}Mn_{35.2}In_{14.8}$ [83]. The giant Hall effect across martensite phase transition with giant Hall angle has been reported in $Ni_{50}Mn_{34.8}In_{15.2}$ MSMA. Recently, AHE has been proposed in $Ni_{50}Mn_{35}In_{15-x}B_x$ (x = 0.5, 0.75) bulk [157] and $Ni_{47.3}Mn_{30.6}Ga_{22.1}$ film [149], but the mechanism behind AHE in these alloys are still not unclear. Therefore, a detailed Hall study is required to explore the mechanism behind AHE and also the possibility of skyrmions in Ni-Mn-based MSMAs.

1.6 Magnetic Shape Memory Alloys with Hexagonal Austenite Phase

Apart from Ni-Mn-based MSMAs with cubic austenite phase, there is another class of materials with hexagonal austenite phase [196], which also shows magnetic shape memory effect (MSME) [197]. These materials are known as Mn-based *MnM′X* compounds, where *M′* is a transition metal element while *X* is a group IIIA or IVA element [198]. Besides MSME, these materials show several other interesting physical properties like magnetocaloric effect [199-201], magnetoresistance [202], noncollinear magnetic structure [203], etc. These interesting properties categories them as potential candidate for wide-ranging technological applications, which include multifunctional sensors/actuators [196, 197], magnetic refrigeration [199-201], and novel memory devices [196, 197, 202]. All these exciting properties are directly related to the presence of unique magnetostructural coupling in the *MnM′X* compounds, wherein a wide range of tunability of ferromagnetic T_C can be achieved by compositional tuning [196, 204]. In general, these materials contain austenite phase with hexagonal structure and martensite phase with lower symmetry structure like orthorhombic [196, 204, 205]. Interestingly, the martensite phase has a higher volume than the austenite phase in these materials [196]. Therefore, the martensite phase in these materials can be suppressed partially to the completely by playing with the composition for chemical pressure tuning [196, 200], creation of sufficient concentration of vacancies [206, 207],

hydrostatic pressure [208], and *e/a* ratio [208]. Thus, there are two classes of materials: one exhibits hexagonal austenite to orthorhombic martensite phase transition and the second one with stable hexagonal austenite phase only. In the recent past, the second class of compounds received tremendous interest as they exhibit exciting skyrmion textures [187, 188, 209], and hence they are the focus of the present thesis.

Moreover, these *MnM′X* compounds are also known as half Heusler-type [210, 211]. In *MnM′X*, consideration of Ni and Ga in place of *M* and *X*, respectively, lead to an exciting MnNiGa [187] compound, which has also been termed as NiMnGa [212]. It is called NiMnGa (instead of MnNiGa) throughout this thesis for simplicity in the discussion. The martensite phase is completely suppressed, and a stable austenite phase with a centrosymmetric hexagonal structure in $P6_3/mmc$ space group is observed in the NiMnGa compound [187, 213, 214]. In the recent past, NiMnGa has received significant attention as it hosts biskyrmions in a wide temperature window (16-340 K) with a high value of the paramagnetic to ferromagnetic (FM) phase transition temperature ($T_C \sim 350$ K) [187, 213, 214]. Biskyrmion is a spin texture of two skyrmions with opposite spin helicities [187]. The large value of T_C (~350 K) and wider temperature stability of biskyrmions make the NiMnGa compound an attractive candidate for a deep investigation to the researchers. Below the FM T_C, NiMnGa exhibits an easy magnetic axis along the *c*-axis of the hexagonal lattice, i.e., uniaxial magnetic anisotropy [214]. In addition to completely random spin arrangements (paramagnetic phase) to ferromagnetically ordered spin-state transition, it exhibits one more interesting magnetic transition within its FM phase that is termed as spin reorientation transition (SRT) [214]. The SRT is related to canting of ferromagnetically aligned spins (collinear) around the *c*-axis and results into the noncollinear spin configuration. The spin canting leads to the appearance of antiferromagnetic (AFM) components in the basal plane of the hexagonal unit cell.

Hence, it exhibits competition between FM and AFM interaction, which is one crucial factor behind biskyrmions formation [214]. The theoretical study proposed that magnetism is dominated by Mn-Mn distance with competing FM and AFM interactions along the *c*-axis in hexagonal NiMnGa [215].

A magnetically originated anomaly in the *c/a* ratio has been observed in hexagonal NiMnGa without any crystallographic symmetry breaking at SRT [214]. This anomaly in the structural parameters (*c/a* ratio) at magnetic transition with preserved crystallographic symmetry is the indication of the presence of magnetoelastic effects [216] or isostructural phase transitions [216, 217]. The magnetoelastic effects deal with the coupling between the magnetic and structural degree of freedom, i.e., it explores how strongly or weakly spin-lattice coupled with each other [218, 219]. The *ab-initio* calculation on magnetoelastic effects in chiral magnetic skyrmions has already been reported [220], which suggests the stability of skyrmions lattice is very sensitive to external mechanical loads or pressure [221-223]. Therefore, a detailed study on magnetoelastic coupling in NiMnGa may provide insight towards understanding the extreme sensitivity of the skyrmionic textures to external stresses as reported in the B20 magnets [220-225].

The manipulation of skyrmions with external pressure provides a bunch of information, which is helpful to improve their functionality [226-228]. In addition, the stability of the hexagonal phase in *MnM′X* compounds stabilize with positive as well as negative chemical pressure, i.e., it is a complex phenomenon that dependents on several factors like size of doping elements, vacancies, valence electron concentration, and local atomic environment [229]. The presence of magnetoelastic coupling may facilitate the formation of the different magnetic structure, which is expected to appear with pressure increasing in NiMnGa, in similar to those has been observed recently for another analogous system (Mn_3Sn), which exhibits hexagonal crystal structure and

topological Hall effects and shows different compression rate in the in-plane and out of plane lattice parameter [230]. Further, applying pressure at room temperature may induce lattice contraction, resulting in reduced interatomic distances. This may result in the stabilization of SRT even at room temperature with pressure, which can be used to maximize the biskyrmions density at room temperature from the 200 K (T_{SRT}). The increasing behavior of T_C with hydrostatic pressure (increasing rate of dT_C/dP ~ 1.7 K/kbar) [231] has been reported for a similar hexagonal sister compound PtMnGa, which hosts Neel-type kyrmions textures with maximum stability at T_{SRT} ~ 215 K [209]. Further, the crystallographic unit cell of NiMnGa contains Mn, Ni, and Ga atoms at 2a, 2d, and 2c Wyckoff sites, respectively [214]. Since Ni and Ga in NiMnGa (similar to Pt and Ga in PtMnGa) have a considerable ratio in their atomic sizes (atomic radii ratio: r_{Ga}/r_{Ni} ~ 0.91 and r_{Ga}/r_{Pt} ~ 0.76), so distortion of the hexagonal unit cell structure on the application of pressure is expected. All these demands a detailed study of hexagonal NiMnGa with external hydrostatic pressure.

The origin of skyrmions has been well understood in the noncentrosymmetric materials due to the presence of DMI [232], but it remains a topic of discussion in the centrosymmetric materials [214, 233]. The NiMnGa has a centrosymmetric hexagonal crystal structure and host biskyrmions [187]. Initially, the crystal structure of PtMnGa, which is a sister compound of NiMnGa, was supposed to be hexagonal in the centrosymmetric $P6_3/mmc$ space group [234]. Recently, a trigonal structure of PtMnGa with a noncentrosymmetric $P3m1$ space group has been proposed using single crystal x-ray diffraction and selected-area electron diffraction studies [209]. This explains the formation of Neel-type skyrmions in PtMnGa [209]. More recently, average structure study of PtMnGa using synchrotron x-ray diffraction and neutron powder diffraction reveals no evidence for the $P3m1$ space group [45]. However, selected-area electron diffraction may provide the information at the

local scale [46]; it is necessary to investigate the local structure of related sister compounds. Local symmetry breaking or structural disorder without long-range ordering in crystalline materials may provide a vital improvement in the exotic physical properties, which can be directly utilized in the technology [235]. Therefore, it is interesting to look the local structure of centrosymmetric NiMnGa to explore the origin of biskyrmions in this alloy system.

1.7 Objective of the Present Work

The Ni-Mn-based MSMAs show several exciting properties (as mentioned in section 1.4), which mainly depend on the interesting phase transitions (including magnetic as well as structural) observed in these alloys. Generally, the martensite phase of Ni-Mn-based MSMAs possesses the modulated structure, which plays a key role behind the appearance of huge MFIS in these alloys. Therefore, it is necessary to understand the phase transitions and crystal structure of different phases to improve the functionality of Ni-Mn-based MSMAs.

The premartensite (PM) phase was thought to be the precursor state of the martensite phase [99, 100] before a recent discovery, which unfolded the robust Bain distorted thermodynamic stable PM phase in $Ni_{1.9}Pt_{0.1}MnGa$ MSMA and proposed that the PM phase should not be considered as the precursor state of the martensite phase [123]. This arose a natural question: is there any precursor state of the PM phase? Although precursor states have been observed in the parent austenite phase in the form of diffuse scattering in Ni_2MnGa MSMA, there is controversy about the origin of these precursors [88, 147]. Thus, a direct structural investigation of such precursors is still required to understand their origin. To explore these precursors, we aim to investigate the local structure of Ni_2MnGa MSMA using high-Q SXRPD data analysis. In addition, the PM phase occurs in the narrow temperature range with weak signature in the conventional experiments. Therefore, a stable PM phase in a wide temperature range is required for depth exploration of the

PM phase and related properties. Our objective is to stabilize the PM phase in the wide temperature range in Ni-Mn-In MSMA by chemical pressure.

It has been observed that the PM phase transition is directly related to the skyrmion formation (and hence, related topological Hall effect) in the Ni-Mn-based MSMAs [83]. Therefore, it is important to investigate the impact of the PM phase on the topological Hall effect (THE) in these alloys. Further, there are only a few reports of the anomalous Hall effect (AHE), whose origin remains a matter of concern, especially in the Ni-Mn-Ga MSMAs, as they exhibit multiple phase transitions (austenite, martensite, and PM phase) [149, 150]. Thus, a detailed study of AHE and THE in Ni-Mn-Ga MSMAs are required to understand the impacts of phase transition on these interesting properties. Our aim is to investigate the origin of anomalous and topological Hall effects in Ni_2MnGa MSMA.

Besides Ni-Mn-based MSMAs, there is another interesting class of MSMAs shows hexagonal austenite to orthorhombic martensite phase transition (see section 1.6). The hexagonal NiMnGa is one of related compounds, and gained significant attention as it shows biskyrmion textures, which can be utilized in the skyrmion-based spintronic devices at higher temperatures [187]. Although temperature dependent structural and magnetic studies are performed [214], a detailed investigation of structural and magnetic correlations is still unclear in NiMnGa. Interestingly, magnetic skyrmions in noncentrosymmetric materials has been proposed to be very sensitive to external loads or pressure due to magnetoelastic coupling [220-225]. Therefore, a detailed study on magnetoelastic coupling in centrosymmetric NiMnGa is expected to provide insight into understanding the biskyrmionic textures' sensitivity to external stresses. We aim to investigate the temperature and pressure dependent phase transition, magnetoelastic coupling, crystal structure, and magnetic correlations in biskyrmion host hexagonal NiMnGa. Recently, a

noncentrosymmetric structure has been observed using electron diffraction studies in PtMnGa [209], and explains the formation of Neel-type skyrmions in PtMnGa [209]. Since PtMnGa is the sister compound of NiMnGa, we aim to investigate the origin of biskyrmions in NiMnGa also.